JOURNAL OF EXPERIMENTAL AND THEORETICAL PHYSICS, 2024, Vol. 165, No. 5, pp. 725–732

STATISTICAL, NONLINEAR, AND SOFT MATTER PHYSICS

BEHAVIOR OF MIXTURES OF ACTIVE AND PASSIVE NEMATICS IN A CONFINED TWO-DIMENSIONAL CIRCULAR DOMAIN

© 2024 L. V. Mirantsev

Institute for Problems in Mechanical Engineering of the Russian Academy of Sciences (IPME RAS)
199178, Saint Petersburg, Russia
e-mail: mlv@ipme.ru

Received October 05, 2023
Revised January 17, 2024
Accepted January 18, 2024

Abstract. Using a simple molecular model of passive, active non-chiral and chiral nematics, molecular dynamics simulations were performed to study the behavior of their binary mixtures in a two-dimensional bounded circular domain. Equilibrium structures in these systems were studied under normal and tangential anchoring of particles at the boundaries. It is shown that in mixtures consisting of passive and active model particles, as well as in mixtures of active particles with different chirality, at sufficiently large self-propelling forces, the bounded domain splits into clusters predominantly consisting of particles of the same type. To characterize the degree of separation of mixtures into these clusters, a segregation parameter is introduced. The values of this parameter are calculated for different magnitudes of selfpropelling forces and chirality of model particles.

DOI: 10.31857/S004445102405e110

1. INTRODUCTION

Active systems are natural or artificial systems that are not in a state of thermodynamic equilibrium due to energy transferred to their constituent particles either externally or through internal chemical processes [1]. Examples of active systems include living creatures (birds, fish, bacteria, etc.). Active systems can also be artificially created from objects using light or chemical energy. The most important feature of active systems is the existence of collective motion, where groups of self-propelled particles move as a single entity on scales significantly exceeding the sizes of individual particles. Studying the mechanism and dynamics of such collective movements is of great importance for researching natural systems across a wide range of scales. Of particular interest are so-called chiral active systems, consisting of particles with broken reflectional symmetry, and especially chiral active nematics, which possess long-range orientational order [2]. Currently, numerous experimental and theoretical studies of chiral active nematics in confined spaces with specified boundary conditions are being conducted. Most theoretical studies of such systems [3-5] have been carried out within the framework of continuum phenomenological models using concepts such as the orientational order tensor $\mathbf{Q}$ and flow velocity field $\mathbf{u}$. These works investigated the spatiotemporal behavior of the director field structure $\mathbf{n}$ and topological defects of active nematics in two-dimensional circular domains at various radii R of these domains and different boundary conditions. The dependence of active nematics behavior on such phenomenological parameters as the active stress strength α was also investigated. However, when considering the behavior of real active systems consisting of microscopic or nanoscopic active particles (for example, suspensions of microtubules and motor proteins [1]), it is quite difficult to correlate the phenomenological parameter α with the characteristics of these particles. Spatial confinement is an important factor determining various properties of active systems, for example, the structure of flows in them and the formation of spiral vortices [3,6-12]. Such confinements can also be used in practical applications, for example, to control living and artificial self-propelled microscopic objects [13-15].

Of particular interest is the behavior of active systems that are mixtures of different active particles

confined in microscopic regions with bounding surfaces [16]. The influence of bounding surfaces can lead to specific behavior of such mixtures. In paper [16], the behavior of a binary mixture of self-propelling and interacting disks with different radii, confined within a two-dimensional square region, was investigated. Using numerical solutions of the Langevin equations describing the motion of these disks, the degree of aggregation of different particles near the bounding walls, as well as their segregation parameter, were obtained. Obviously, such a model is quite far from a more or less plausible model of active nematics consisting of self-propelling particles with elongated shapes. It is also impossible to use it to investigate the behavior of orientational order in mixtures of such particles.

In works [17, 18] we proposed a rather simple microscopic model of active chiral nematics, and using molecular dynamics (MD) simulation, their behavior in two-dimensional circular and ring-shaped confined regions with various boundary conditions was investigated. It was shown that at not very large active self-propelling forces acting on particles in such systems, their structure and the arrangement of topological defects qualitatively coincide with the results of the aforementioned phenomenological models [3-5]. In this regard, we used the same model for MD simulation of the behavior of binary mixtures of active and passive nematics, as well as mixtures of active nematics with different chirality in a two-dimensional circular region with bounding surfaces with normal and tangential anchoring of particles with them. The dependence of this behavior on the geometric and force characteristics of model particles was investigated.

2. MODEL

For active nematic particles, very simple models were used, as shown in Fig. 1.

The isotropic part of the interaction between particles of the considered active and passive nematic is described using a short-range Lennard-Jones (LJ) pair potential

$$U_{LJ}(r_{ij}) = 4\varepsilon\left[\left(\frac{\sigma}{r_{ij}}\right)^{12} - \left(\frac{\sigma}{r_{ij}}\right)^{6}\right], \qquad (1)$$

which was used in our earlier works [19-21]. Here ε and σ — are the energy constant and characteristic length of LJ-interaction between ith and jth particles, r_{ij} — is the distance between them. The anisotropic part of the interaction between these particles is described by the following Maier-Saupe type potential:

$$U_{anis}(r_{ij}, \theta_{ij}) = -\varepsilon_{anis}\left(\frac{3}{2}\cos^2\theta_{ij} - \frac{1}{2}\right)\frac{\sigma^6}{r_{ij}^6}, \qquad (2)$$

where ε_{anis} — is the energy constant of anisotropic interaction, θ_{ij} — is the angle between the long axes of ith and jth particles. The interaction between mixture particles and boundaries of the two-dimensional circular region in which it is placed is also described by potentials similar to potentials (1) and (2), where interaction constants ε, ε_{anis} and σ are replaced with interaction constants ε_2, ε_{anis2} and σ_2. Additionally, each active particle is affected by a selfpropelling reactive force $\mathbf{f}_0$, with components along axes x and y equal to

$$f_{0x} = f_0 e_x \cos\phi + f_0 e_y \sin\phi, \qquad (3)$$

$$f_{0y} = f_0 e_y \cos\phi - f_0 e_x \sin\phi, \qquad (4)$$

where $\mathbf{e}$ — is a unit vector directed along the particle's long axis, φ — is the angle between $\mathbf{e}$ and $\mathbf{f}_0$. Furthermore, in the case of chiral particles, the self-propelling reactive force $\mathbf{f}_0$ creates an additional torque $\tau_0 = f_0\delta\sin\phi$ relative to its center of mass. For non-chiral particles, the angle φ in formulas (3) and (4) must be set to zero, and the additional torque is simply absent. The position in space and orientation of the ith particle of active or passive nematic were determined by numerically solving the following equations of motion:

$$\frac{\partial^2 \mathbf{r}_i}{\partial t^2} = \frac{\mathbf{f}_i}{m}, \qquad (5)$$

$$\frac{\partial \mathbf{e}_i}{\partial t} = \omega_i \times \mathbf{e}_i, \qquad (6)$$

$$\partial\omega_i / \partial t = \tau_i / I. \qquad (7)$$

Here $\mathbf{f}_i$ and τ_i — are total force and total moment acting on the ith particle from other particles on the confining surface, as well as self-propelling force and moment; $\boldsymbol{\omega}_i$ — is angular velocity of vector rotation $\mathbf{e}_i$; m and I — are mass and moment of

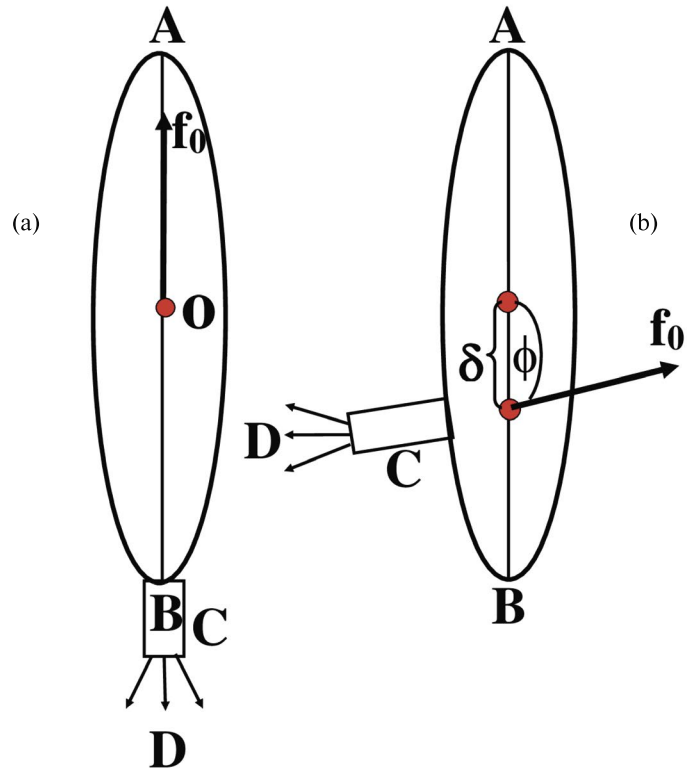

Fig. 1. Models of non-chiral (*a*) and chiral (*b*) particles of active nematic used in our MD simulation: AB — long axis of particles; O — their center of mass; C — protrusion providing particles' self-propulsion ability (lateral protrusion provides its chirality); D — a jet ejected from this protrusion resulting in the self-propelling reactive force $\mathbf{f}_0$ (in case of chiral particle, it is applied at point O_1 and directed at angle φ to the particle's long axis); δ — distance between the force application point $\mathbf{f}_0$ and particle's center of mass

inertia of the particle respectively. MD simulation was performed on NVT ensembles, and at each time step, the equations of motion were solved using standard algorithm [22], and the reduced system temperature T / ε was maintained constant at 0.9 using thermostat [22]. To describe the orientational order of particles inside the circular region, we introduced radial Q_R and tangential Q_T order parameters, which were defined as

$$Q_R = \frac{1}{N}\sum_i | \mathbf{e}_i \cdot \hat{\mathbf{r}}_i |, \tag{8}$$

$$Q_T = \frac{1}{N}\sum_i | \mathbf{e}_i \cdot \mathbf{n}_i |, \tag{9}$$

where N — is the total number of particles inside the circular region, $\hat{\mathbf{r}}_i$ and $\mathbf{n}_i$ — are unit vectors parallel and perpendicular to the radius vector of the $\mathbf{r}_i$ ith particle. Additionally, to determine the segregation degree of different types of nematic particles (active non-chiral, active chiral, passive), we introduced segregation parameter S, which was defined as follows. The two-dimensional region containing mixture of different particles was divided into N_1 sufficiently small subregions and for each kth region, parameter

$$S_k = | n_{k1} - n_{k_2} | /(n_{k1} + n_{k2}), \tag{10}$$

was calculated where n_{k1} and n_{k2} — are numbers of particles of first and second type respectively in this kth region. Then the segregation parameter S for the entire system is defined as

$$S = \frac{1}{N_1}\sum_k S_k, \tag{11}$$

where summation is performed over all N_1 subregions.

3. RESULTS OF MD SIMULATION AND THEIR DISCUSSION

We conducted MD simulation of a system consisting of 1,820 particles confined within a two-dimensional circular region with radius 24σ. Half

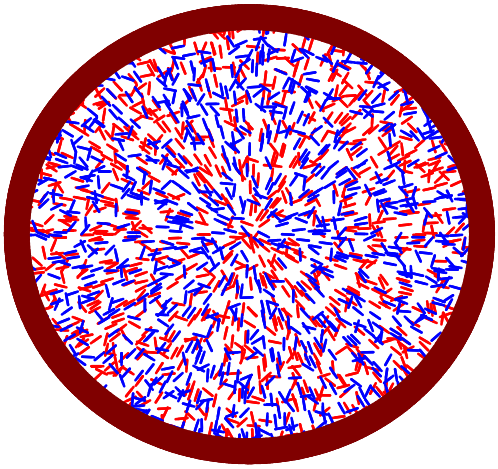

Fig. 2. Initial configuration for MD simulation of binary mixtures behavior inside a two-dimensional circular region. Red and blue dashes represent particles of type 1 and 2 respectively, brown ring-shaped area contains ghost particles

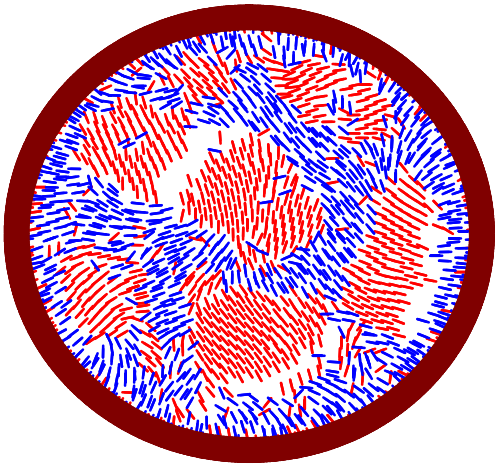

Fig. 3. Configuration of binary mixture containing 50% active particles with $f_0 = 10$, $\phi = \pi / 2$ and 50% passive particles with $f_0 = 0$, under boundary conditions with normal anchoring at $t = 100$ (values are given in dimensionless MD units [22])

of the particles were type l, particles, and the other half were type 2 particles. The boundary conditions in such a system were set using "ghost" particles forming a layer with thickness 2σ at the boundary of the considered circular region. These particles were considered immobile and oriented so that their unit vectors e were directed along the radius drawn from the center of the circular region to the location point of the given ghost particle

We considered two types of boundary conditions corresponding to strong tangential and normal anchoring on the confining surface. In the first case,

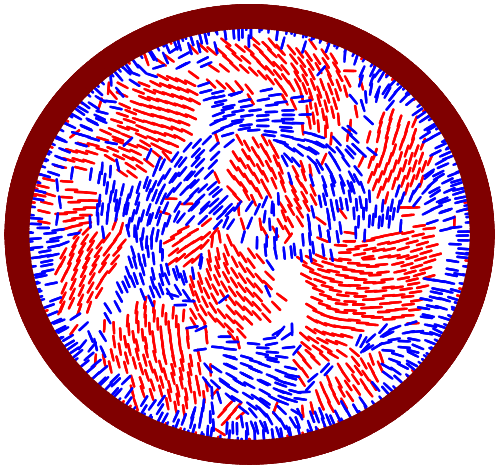

Fig. 4. The same configuration of binary mixture as in Fig. 3, but with $f_0 = 30$

ghost particles induce the orientation of nematic particles along the tangent to the boundary, and in the second case – along the radius drawn to a given point. To ensure strong tangential anchoring, the interaction constant ε_2 between nematic particles and the boundary of the two-dimensional circular region (i.e., ghost particles) was considered equal to -5ε, and for strong normal anchoring we took $\varepsilon_2 = 5\varepsilon$. We also assumed that ε, σ_i, m, I and δ are simply equal to one in dimensionless MD units [22]. In all cases, the simulation started from the initial configuration (Fig. 2), where particles were randomly positioned inside the circular region and had random orientations of their long axes.

First of all, we conducted MD simulation of a binary mixture consisting half of active particles with protrusion C in Fig. 1*b*, directed at an angle $\phi = \pi / 2$ to the long axis of the particle, while the second half of the mixture was a regular "passive" nematic (force $f_0 = 0$). Fig. 3 shows the configuration of such mixture at $f_0 = 10$, with normal anchoring boundary conditions and at $t = 100$. It can be seen that the mixture inside the circular region consists of small clusters containing mainly particles of either the first or second type, however, the boundaries between them are not sharp. The presence of small rarefied areas between some clusters can be explained by the fact that the particle density in clusters is slightly higher than the average density of uniformly distributed particles in the initial configuration shown in Fig. 2. The separation into clusters consisting of active

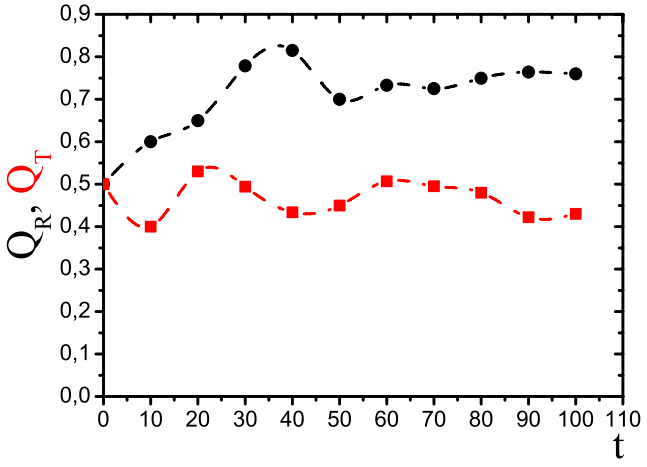

Fig. 5. Time dependencies of parameters Q_R (*1*) and Q_T (*2*), starting from the moment $t = 0$, which corresponds to the initial configuration in Fig. 2, and ending at the moment $t = 100$, corresponding to the configuration in Fig. 4

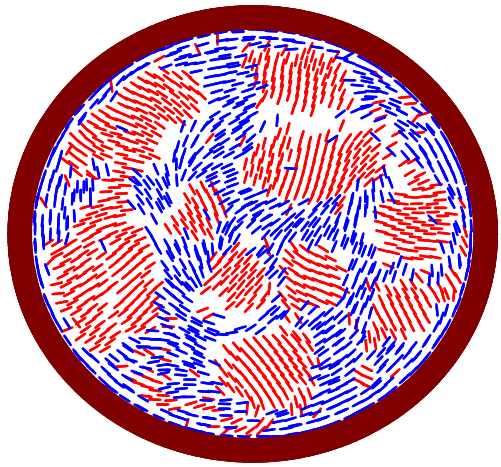

Fig. 7. Configuration of the binary mixture at $t = 100$ under boundary conditions with tangential anchoring. $f_0 = 30$

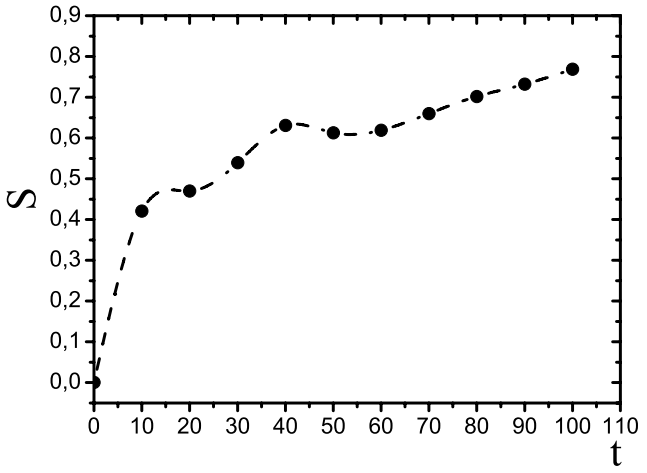

Fig. 6. Time dependence of parameter S for a binary mixture containing 50 % active particles with $f_0 = 30$, $\phi = \pi / 2$ and 50 % passive particles with $f_0 = 0$, under boundary conditions with normal anchoring

and passive particles becomes more distinct with increasing self-propelling force f_0. This is clearly visible in Fig. 4, which shows the configuration of the same mixture and under the same boundary conditions, but at $f_0 = 30$.

Fig. 5 shows the time dependencies of the order parameters Q_R and Q_T for the abovementioned mixture, and Fig. 6 shows the time dependence of the corresponding segregation parameter S. In Fig. 5, it can be seen that the dependencies Q_R and Q_T start from the same value $Q_R = Q_T = 0.5$, which corresponds to the initial configuration at $t = 0$, shown in Fig. 2, where the orientations of both active and passive particles are randomly distributed. The further increase in parameter Q_R and decrease in parameter Q_T are caused by boundary conditions with normal anchoring, which makes radial orientational order more preferable.

When calculating the segregation parameter we divided the circular region containing our binary mixture into 10 rings of equal thickness, and then divided each ring into 24 equal sectors, thus obtaining 240 sufficiently small subregions. After that, the procedure for determining the parameter S described in Section 2, was carried out. Its result, shown in Fig. 6, indicates a gradual increase in the segregation parameter from zero, which corresponds to the initial configuration with random distribution of active and passive particles inside the circular region, to a rather large value $S \approx 0.75$, corresponding to the configuration with clusters in Fig. 4. With further simulation ($t > 100$) the segregation parameter practically does not increase, indicating saturation.

Fig. 7 shows the configuration of our mixture at $t = 100$ under boundary conditions with tangential anchoring at $f_0 = 30$. This configuration also contains clusters of active and passive particles, similar to the clusters in Fig. 4. The dependence of order parameters Q_R and Q_T under such boundary conditions is similar to the dependence of these parameters in Fig. 5, but these parameters seem to swap places, i.e., Q_T increases while Q_R decreases.

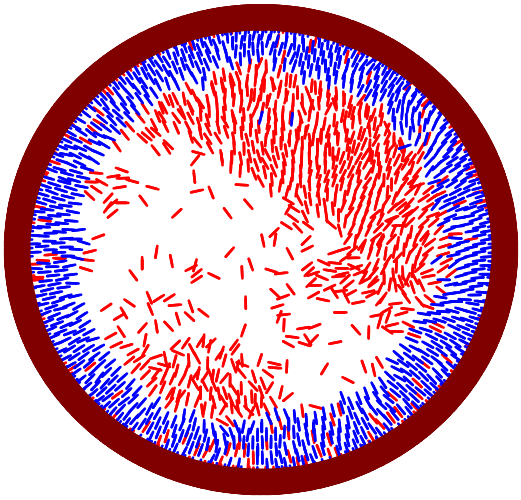

Fig. 8. Configuration of a binary mixture containing 50% active particles with $f_0 = 30$, $\phi = \pi / 2$ and 50% active particles with $f_0 = 30$, but without chirality ($\phi = 0$) under boundary conditions with normal anchoring at $t = 100$

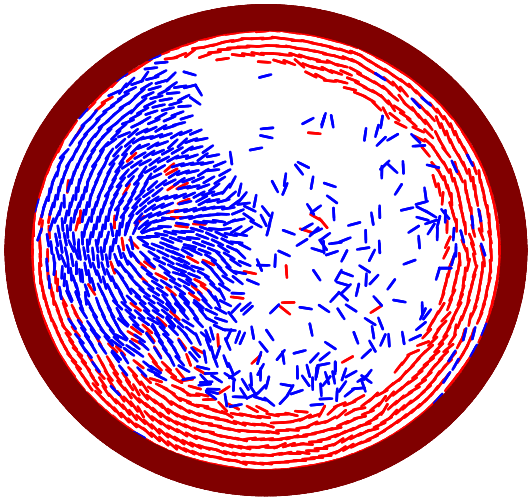

Fig. 10. Configuration of the same binary mixture as in Fig. 8, but with tangential anchoring boundary conditions $t = 100$

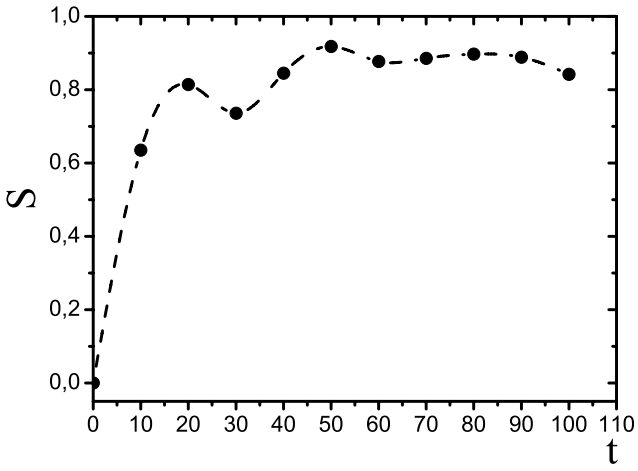

Fig. 9. Time dependence of parameter S for a binary mixture of active particles with different chirality (50% $f_0 = 30$, $\phi = \pi / 2$ and 50% $f_0 = 30$, $\phi = 0$) under boundary conditions with normal anchoring

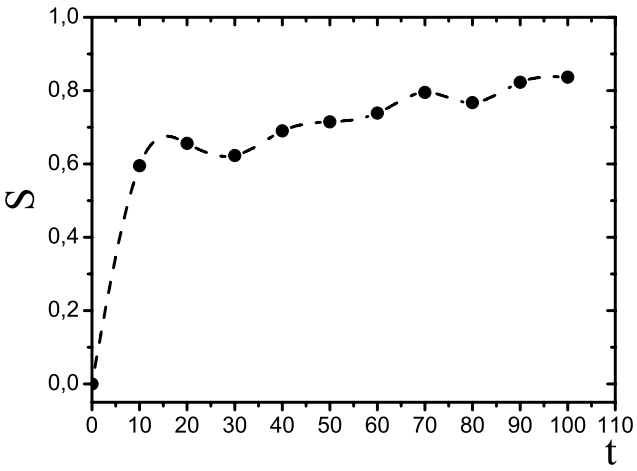

Fig. 11. Time dependence of the parameter S for a binary mixture of active particles with different chirality (50% $f_0 = 30$, $\phi = \pi / 2$ и 50% $f_0 = 30$, $\phi = 0$) under tangential anchoring boundary conditions

This is also caused by boundary conditions with tangential anchoring, making tangential orientational order more preferable.

Regarding the segregation parameter S, its time dependence under tangential anchoring is similar to the time dependence in Fig. 6, and its value at $t = 100$ is also approximately equal to 0.75. These results indicate that at a sufficiently large value of self-propelling force $f_0 = 30$ there is a rather clear separation of the binary mixture into clusters of active and passive particles, weakly dependent on boundary conditions.

MD simulation was also conducted to study the behavior of binary mixtures of active particles with different chirality under boundary conditions with normal and tangential anchoring. In particular, Fig. 8 shows the configuration of a binary mixture containing 50% active particles with $f_0 = 30$ and $\phi = \pi / 2$ and 50% active particles with $f_0 = 30$, but without chirality ($\phi = 0$), under boundary conditions with normal anchoring at $t = 100$. In Fig. 8, it can be seen that this binary mixture splits into two large clusters, one of which consists of normally oriented active particles with zero chirality

and forms a ring-shaped region near the confining surface. The second large cluster consists of active particles with angle $\phi = \pi / 2$ and adjoins the right half of the clusster consisting of active particles with zero chirality. There is also a small cluster of active chiral particles adjacent to the left half of the ring-shaped cluster of active non-chiral particles, and a rarefied region with active chiral particles. The above-described procedure for determining the segregation parameter S gives its time dependence, shown in Fig. 9. It can be seen that at $t = 0$ (initial configuration in Fig. 2) the parameter S equals zero and at $t = 100$ (configuration in Fig. 8) it reaches quite a large value $S \approx 0.9$.

Fig. 10 shows the configuration of a similar binary mixture, but with tangential anchoring boundary conditions. It can be seen that active chiral particles ($\phi = \pi / 2$) with tangential orientation in this case form a ring-shaped cluster near the confining surface, while active nonchiral particles ($\phi = 0$) form a large cluster adjacent to the left part of this ring-shaped region, as well as a rarefied area with low particle concentration. The corresponding time dependence of the segregation parameter is shown in Fig. 11. This dependence is very similar to the analogous dependence in Fig. 9 for the case of the same binary mixture under normal anchoring boundary conditions. Both dependencies at $t = 100$ have a segregation parameter value of $S = 0.8–0.9$. This indicates that in a binary mixture of active particles with different chirality, confined within a circular region, there is also separation into clusters consisting of particles of the same type, weakly dependent on boundary conditions.

4. CONCLUSION

MD simulation of the behavior of binary mixtures of model active and passive nematics, as well as active nematics with different chirality inside a two-dimensional circular region with confining surfaces with normal and tangential anchoring has been conducted.. These model active materials consist of elongated particles that interact through an isotropic Lennard-Jones potential and an anisotropic Maier-Saupe type potential. Such elongated particles also have appendages that emit a jet of some substance, created due to some internal chemical reaction. In the case of non-chiral particles, these appendages are located at the end of elongated particles and directed along their long axes. In chiral particles, the appendages are located on the side and form some angle φ with the long axes. As a result, in the case of non-chiral particles, the emitted jet creates an additional reactive self-propelling force $\mathbf{f}_0$, directed along the long axes of the particles, while chiral particles are affected not only by the reactive selfpropelling force but also by an additional torque τ_0, that causes self-rotation of particles relative to their geometric centers. For passive nematics, the self-propelling force $\mathbf{f}_0$ and additional torque τ_0 are zero. It was found that a binary mixture of active and passive nematics, confined within a circular region, regardless of boundary conditions, breaks up into separate clusters consisting mainly of particles of one type, and the larger the self-propelling force $\mathbf{f}_0$, the more distinct such cluster structure appears. The same clustering occurs in mixtures of active nematics with different chirality. For each binary mixture, the segregation parameter S for its particles was calculated and it was shown that the value of this parameter can reach quite a large value $S = 0.8–0.9$.

REFERENCES

1. 1. C. Bechinger, R. Di Leonardo, H. Lowen, C. Reichhardt, and G. Volpe, Rev. Mod. Phys. 88, 045006 (2016).
2. A. Doostmohammadi, J. Ignes-Mullo, J. Yeomans, and F. Sagues, Nat. Commun. 9, 3246 (2018).
3. M. Norton, A. Baskaran, A. Opathalage, B. Langeslay, S. Fraden, A. Baskaran, and F. Hagan, Phys. Rev. E 97, 012702 (2018).
4. A. Maitra and M. Lenz, Nat. Commun. 10, 920 (2019).
5. M. Norton, P. Grover, M. Hagan, and S. Fraden, Phys. Rev. Lett. 125, 178005 (2020).
6. H. Wioland, F. G. Woodhouse, J. Dunkel, J. O. Kessler, and R.E. Goldstein, Phys. Rev. Lett. 110, 268102 (2013).
7. H. Wioland, E. Lushi, and R. E. Goldstein, New J. Phys. 18, 075002 (2016).
8. M. Ravnik and J. M. Yeomans, Phys. Rev. Lett. 110, 026001 (2013).
9. A. Doostmohammadi and J. M. Yeomans, Eur. Phys. J. Spec. Top. 227, 2401 (2019).
10. S. Rana, M. Samsuzzaman, and A. Saha, Soft Matter 15, 8865 (2019).
11. 1S. Das and R. Chelakkot, Soft Matter 16, 7250 (2020).
12. S. Das, S. Ghosh, and R. Chelakkot, Phys. Rev. E 102, 032619 (2020).

13. S. Das, A. Garg, A. I. Campbell, J. Howse, A. Sen, D. Velegol, R. Golestanian, and S. J. Ebbens, Nat. Commun. 6, 8999 (2015).

14. T. Ostapenko, F. J. Schwarzendahl, T. J. Boddeker, C. T. Kreis, J. M. Cammann, G. Mazza, and O. Baumchen, Phys. Rev. Lett. 120, 068002 (2018).

15. M. Popescu, S. Dietrich, and G. Oshanin, J. Chem. Phys. 130, 94702 (2009).

16. X. Yang, M. L. Manning, and M. C. Marchetti, Soft Matter 10, 6477 (2014).

17. L. V. Mirantsev, Eur. Phys. J. E 44, 112 (2021).

18. E. J. L. de Oliveira, L. V. Mirantsev, M. L. Lyra, and I. N. de Oliveira, J. Mol. Liq. 377, 121513 (2023).

19. A. K. Abramyan, N. M. Bessonov, L. V. Mirantsev, and N.A. Reinberg, Phys.Lett. A 379, 1274 (2015).

20. A. K. Abramyan, N. M. Bessonov, L. V. Mirantsev, and A. A. Chevrychkina, Eur. Phys. J. B 9148 (2018).

21. L. V. Mirantsev, Phys. Rev. E 100, 023106 (2019).

22. M. P. Allen and J. Tildesly, Computer Simmulations of Liquids, Clarendon Press, Oxford (1989).